

# Water-stable organic transistors and their application in chemical and biological sensors

Mark E. Roberts\*, Stefan C. B. Mannsfeld\*, Núria Queraltó\*†, Colin Reese\*, Jason Locklin\*, Wolfgang Knoll†, and Zhenan Bao\*\*

\*Department of Chemical Engineering, Stanford University, Stauffer III, 381 North-South Mall, Stanford, CA 94305; and †Max Planck Institute for Polymer Research, Ackermannweg 10, D-55128 Mainz, Germany

Edited by Nongjian Tao, Arizona State University, Tempe, AZ, and accepted by the Editorial Board June 18, 2008 (received for review March 3, 2008)

**The development of low-cost, reliable sensors will rely on devices capable of converting an analyte binding event to an easily read electrical signal. Organic thin-film transistors (OTFTs) are ideal for inexpensive, single-use chemical or biological sensors because of their compatibility with flexible, large-area substrates, simple processing, and highly tunable active layer materials. We have fabricated low-operating voltage OTFTs with a cross-linked polymer gate dielectric, which display stable operation under aqueous conditions over  $>10^4$  electrical cycles using the p-channel semiconductor 5,5'-bis-(7-dodecyl-9H-fluoren-2-yl)-2,2'-bithiophene (DDFTF). OTFT sensors were demonstrated in aqueous solutions with concentrations as low as parts per billion for trinitrobenzene, methylphosphonic acid, cysteine, and glucose. This work demonstrates of reliable OTFT operation in aqueous media, hence opening new possibilities of chemical and biological sensing with OTFTs.**

organic semiconductors | low-voltage | polymer dielectric | chemical detection

The development of portable, robust organic thin-film transistor (OTFT)-based sensors functional in aqueous systems still faces many challenges, despite their vast potential in the health industry, environmental monitoring (1), and national defense (2). Ideally, expensive labeling and detection equipment can be eliminated with a simple device capable of transducing a binding event into an easily deciphered electrical signal (3, 4). OTFTs provide an ideal platform for inexpensive, single-use chemical or biological sensors (5–7). In addition to their inherent advantages of compatibility with flexible, large-area substrates, the properties of organic materials are highly tunable for chemical sensitivity and easily modified with receptor sites for specific interactions. The ability to control the film morphology provides yet another degree of versatility, directly influencing the pathway for analyte molecules to the transistor-critical semiconductor–dielectric interface (8). Previously, the use of OTFTs as sensors had been limited to vapor sensing (9, 10) or after exposure to a solution (11).

In the vapor phase, OTFTs have shown sensitivity to a variety of solvent vapors as observed through a change in the transistor current upon exposure to the analyte (9, 10). The mechanism for vapor sensing has been attributed to analytes diffusing into grain boundaries causing either trapping or doping of charge carriers (3, 12, 13). To achieve selectivity, a “fingerprint” approach has been demonstrated, where an array of semiconductors are used to identify an analyte based on a pattern of responses (9). More recent work, however, has shown that proper modification of the semiconductor material can lead to more directed responses. For example, Huang *et al.* (14) incorporated alkoxy side chains in an organic semiconductor layer and observed an improved response to phosphonate vapors compared to the alkyl-substituted material. Additionally, semiconductors modified with chiral, non-racemic amino acid groups were used for discrimination between citronellol enantiomers (15).

OTFTs reported to date have not been suitable for aqueous systems because of high operating voltages, degradation, and

delamination under aqueous conditions (16). Furthermore, OTFT operation in humid environments has been shown to significantly degrade the performance of these devices, especially when using reactive materials such as pentacene (17). Additionally, it is unknown whether the presence of ionic current will make it impossible for OTFTs to detect chemical species in water. It is noted that sensing in electrolytes has been demonstrated by using variations of the traditional OTFT structure, such as the ion-sensitive organic field-effect transistor (ISOFET) (18) and the organic electrochemical transistor (OEFT), which have previously been reviewed (7). In these sensor devices, however, the current is modulated by electrochemical doping or de-doping processes (OEFT), oxidation-reduction reactions, or ion transport in the electrolyte solution (ISOTFT).

In this report, we demonstrate robust, low-voltage OTFTs that are capable of stable operation in aqueous media enabling a new generation of sensing applications. These OTFTs, based on a thin, cross-linked gate dielectric and a stable organic semiconductor, were used to detect changes in pH and low concentrations of chemicals, such as trinitrobenzene, cysteine, methylphosphonic acid, and glucose in water. Low-voltage transistor operation is critical to stable operation in aqueous media to avoid electrolytic hydrolysis of water and high ionic conduction through the analyte solution. Furthermore, consideration must be given to the selection of the organic semiconductor to accommodate performance and stability requirements in aqueous solutions.

Low-voltage transistor operation has attracted interest for reasons other than operation in aqueous media, particularly for low-power applications. Notable advances include the incorporation of ultrathin, cross-linked polymer gate dielectric layers, such as divinyltetramethylsiloxane-bis(benzocyclobutene) (BCB) (19) or poly(4-vinylphenol) (PVP) cross-linked with trichlorosilanes (20). Self-assembled monolayer and multilayer dielectrics have also been used to achieve low-voltage operation (21, 22) and low-power complimentary circuits (23). These, among other methods of achieving low-power OTFT operation, could potentially be useful in OTFT sensor devices. With the demonstration of robust, high-performance OTFTs that are capable of detecting parts per billion (ppb) analyte concentrations in water, we have overcome a substantial hurdle for the realization of cheap and mass-produced aqueous sensors.

## Results and Discussion

As described above, several ultrathin dielectric materials have been reported for OTFTs. Here, we choose to incorporate a

Author contributions: M.E.R., W.K., and Z.B. designed research; M.E.R., S.C.B.M., and N.Q. performed research; M.E.R., C.R., and J.L. contributed new reagents/analytic tools; M.E.R. and S.C.B.M. analyzed data; and M.E.R. and Z.B. wrote the paper.

The authors declare no conflict of interest.

This article is a PNAS Direct Submission. N.T. is a guest editor invited by the Editorial Board.

\*To whom correspondence should be addressed. E-mail: zbao@stanford.edu.

This article contains supporting information online at [www.pnas.org/cgi/content/full/0802105105/DCSupplemental](http://www.pnas.org/cgi/content/full/0802105105/DCSupplemental).

© 2008 by The National Academy of Sciences of the USA

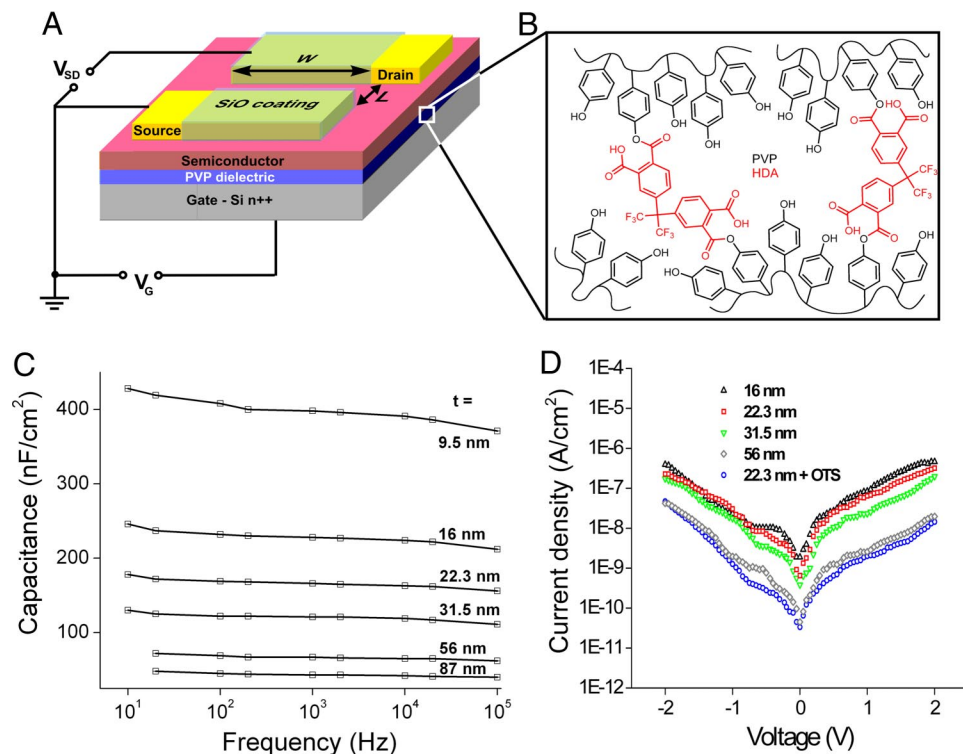


**Fig. 1.** Cross-linked polymer gate insulator and its corresponding electrical properties. (A) Structure of the top-contact OTFT sensor. (B) Chemical structure of cross-linked PVP with HDA. (C) Capacitance vs. frequency. (D) Leakage current vs. voltage for various PVP-HDA films.

cross-linked polymer dielectric because of its simplicity in formulation and deposition. We developed a new cross-linkable polymer dielectric layer with high stability toward air and moisture and low-temperature cross-linking.

The polymer matrix for the gate dielectric layer in this study is poly(4-vinylphenol) (PVP), selected for its proven compatibility with various organic semiconductors (20, 24, 25). Moreover, its hydroxyl groups are well suited for cross-linking with commercially available, ambient-stable cross-linkers, such as 4,4'-(hexafluoroisopropylidene)diphthalic anhydride (HDA) and suberoyl chloride (SC). A catalytic amount of triethylamine is required to promote the cross-linking reaction with HDA. A schematic of the polymer system is shown in Fig. 1B. Solutions of PVP-HDA and PVP-SC in propylene glycol monomethyl ether acetate (PGMEA) were stable for many weeks with no visible precipitation or cloudiness. Thin insulating films were deposited by spin-coating and cured at 100°C, yielding highly uniform pinhole free layers with a surface roughness of 0.2–0.3 nm [supporting information (SI) Fig. S1], as determined by atomic force microscopy (AFM).

Dielectric films of various thicknesses were electrically characterized in sandwich electrode structures with gold pads (0.9, 0.2, and 0.09 mm<sup>2</sup>) on the surface of polymer films on highly doped silicon substrates. The dielectric films exhibited a high capacitance of up to 400 nF/cm<sup>2</sup> (10 nm PVP-HDA), as shown in Fig. 1C. For OTFT characterization, however, we used 22-nm PVP-HDA films with a capacitance of 165 nF/cm<sup>2</sup>. The dielectric constant of 4.2 was determined from the slope of capacitance vs. inverse thickness (at each frequency). These films showed low leakage currents of <10<sup>-6</sup> A/cm<sup>2</sup> and 10<sup>-8</sup> A/cm<sup>2</sup> for 22- and 56-nm films, respectively, for biases below 2 V.

The p-channel semiconductors pentacene, 5,5'-bis-(7-dodecyl-9H-fluoren-2-yl)-2,2'-bithiophene (DDFTTF) (26, 27), and copper(II) phthalocyanine (CuPc), and an n-channel copper(II) 1,2,3,4,8,9,10,11,15,16,17,18,22,23,24,25-

hexadecafluoro-29H,31H-phthalocyanine (FCuPc) were thermally evaporated onto PVP-HDA (22 nm)-coated substrates. Top-contact OTFTs of each material exhibited excellent linear and saturation regime characteristics at low operating voltages. OTFTs fabricated with pentacene (40 nm) showed exceptional device characteristics with a mobility of 1.5 cm<sup>2</sup>/Vs and an on/off ratio of 5 × 10<sup>4</sup> at a gate bias of 1 V. When the dielectric layer was modified with octadecyltriethoxysilane (OTS), the pentacene OTFTs achieved a mobility as high as 3 cm<sup>2</sup>/Vs and an on/off ratio of 10<sup>6</sup> at 2 V (Fig. 2A). DDFTTF (40 nm) showed a mobility as high as 0.39 cm<sup>2</sup>/Vs (0.2 cm<sup>2</sup>/Vs average) and an on/off ratio of 2 × 10<sup>5</sup> (Fig. 2B). FCuPc also performed well at a gate bias of 2 V with a mobility of 0.045 cm<sup>2</sup>/Vs and an on/off ratio of >10<sup>3</sup>. Additional OTFT characteristics are available in SI Text and Figs. S1–S10.

The chemical robustness of the PVP-HDA film was corroborated by drop-casting soluble oligothiophenes from a bromobenzene solution at 90°C under a saturated vapor (28). After solvent evaporation and removal under vacuum, top-contact OTFTs were fabricated on the highly crystalline semiconductor thin films of trimethyl-[2,2';5',2'';5'',2''']quaterthiophen-5-ylsilane (4TTMS) and 5,5'''-dicyclohexyl-[2,2';5',2'';5'',2''']quaterthiophene (CH4T) (29) exhibiting mobilities as high as 0.08 cm<sup>2</sup>/Vs and 0.025 cm<sup>2</sup>/Vs, respectively, and on/off ratios of >2 × 10<sup>3</sup> at 1 V.

OTFT operation under aqueous conditions was characterized using OTFT with PVP-HDA (22 nm) and DDFTTF (40 nm) films without any protective coating or encapsulation covered by a drop of distilled water. The applied source-drain bias was limited to below -0.6 V to reduce the influence of ionic conduction through the analyte solution on the measured drain current. In ambient, we observed ideal device characteristics for |V<sub>DS</sub>| and |V<sub>G</sub>| ~ 0.6 V, as shown by the black curves in Fig. 3B. After exposing the channel to water, we observed a positive shift in threshold voltage and an increase in both the on- and

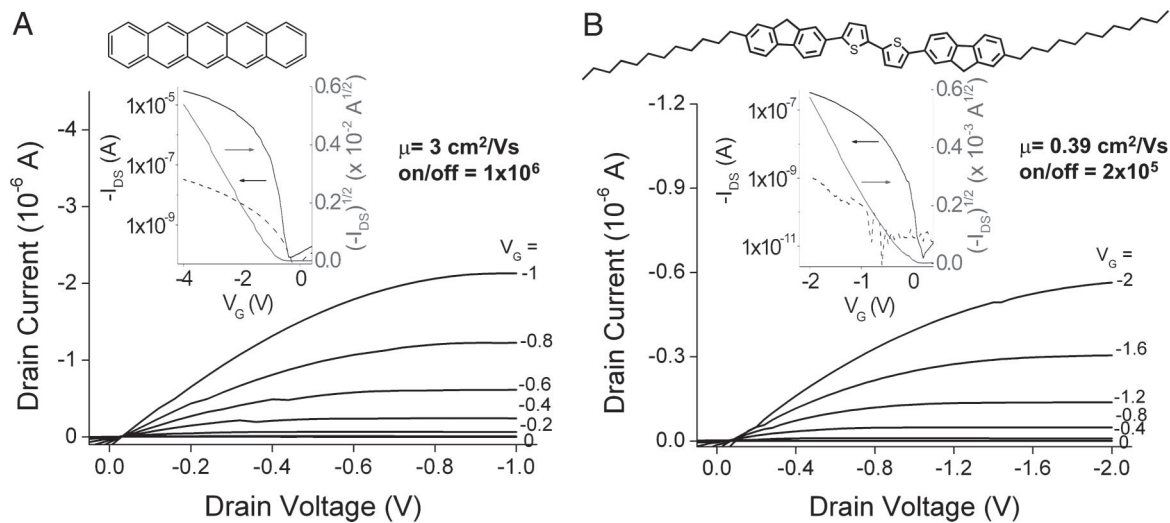


**Fig. 2.** Electrical characteristics of p-channel OTFTs with a PVP-HDA insulator layer and a source-drain electrode geometry of  $W/L = 20$ . Output and transfer (inset) characteristics of OTFTs with 40-nm thermally evaporated films of pentacene on OTS (A) and DDFTTF (B). The gate current is shown in dashed lines.

off-current, illustrated by the red curve. Fig. 3C shows the mobility and threshold voltage shift that occurs within the first 2–3 min as water penetrates the film. Remarkably, the transistor still functioned well in water without any encapsulation. Similar doping effects by moisture have been reported for polythiophene and pentacene films on a hygroscopic dielectric (30, 31). The output characteristics in ambient and under water are shown in Fig. 3D and E, respectively.

Long-term operational stability was demonstrated by cycling the gate bias between 0.3 and  $-1$  V for  $>10^4$  cycles with a

constant source-drain bias,  $V_{DS} = -0.6$  V, while the entire OTFT was exposed to water. Fig. 3E shows the transistor  $I_{DS}$  as a function of  $V_G$  cycle for an OTFT with DDFTTF, with the first 20 cycles expanded for clarity. After  $10^4$  cycles, the apparent mobility and on/off ratio changed from  $0.29$   $\text{cm}^2/\text{Vs}$  to  $0.28$   $\text{cm}^2/\text{Vs}$  and 147 to 151, respectively, while the threshold voltage remained unchanged at  $0.24$  V.

In addition to DDFTTF, similar derivatives, such as dihexyl-FITTF and FITTF, also showed stable operation under water. Some other organic semiconductors showed field-effect in the

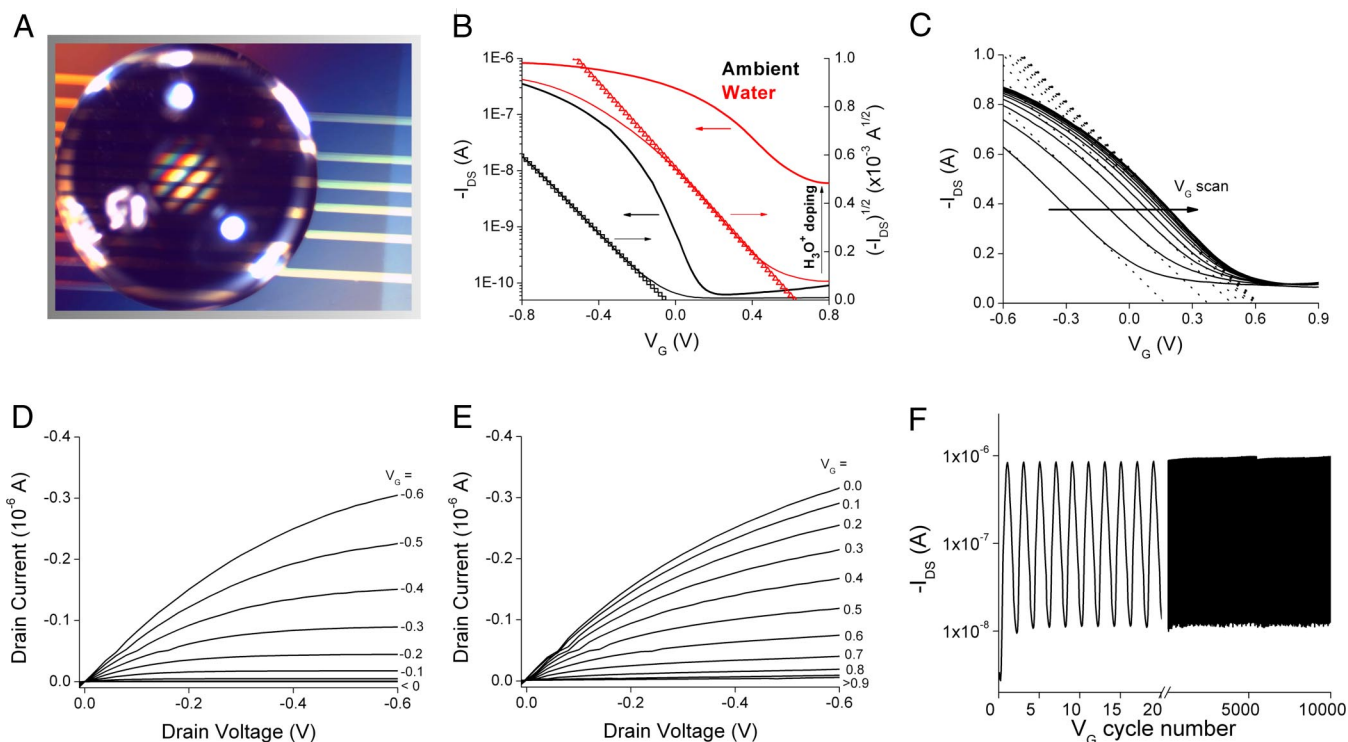


**Fig. 3.** DDFTTF OTFT operation in aqueous media. (A) Optical micrograph of an OTFT with DDFTTF and 22-nm PVP-HDA under aqueous conditions. (B) Transfer characteristics ( $V_{DS} = -0.6$  V) in ambient (black) and water (red). The right axis shows the semilog plot of  $I_{DS}$  vs.  $V_G$  and the left axis shows  $I_{DS}^{1/2}$  vs.  $V_G$ . (C) Transfer characteristics recorded sequentially after the addition of water. (D) Output characteristics ( $I_{DS}$  vs.  $V_{DS}$ ) in ambient. (E) Output characteristics under water. (F)  $I_{DS}$  vs.  $V_G$  (0.3 to  $-1$  V) at a  $V_{DS} = -0.6$  V measured over  $10^4$  cycles (over a period of 12 h) with the initial 20 cycles expanded.

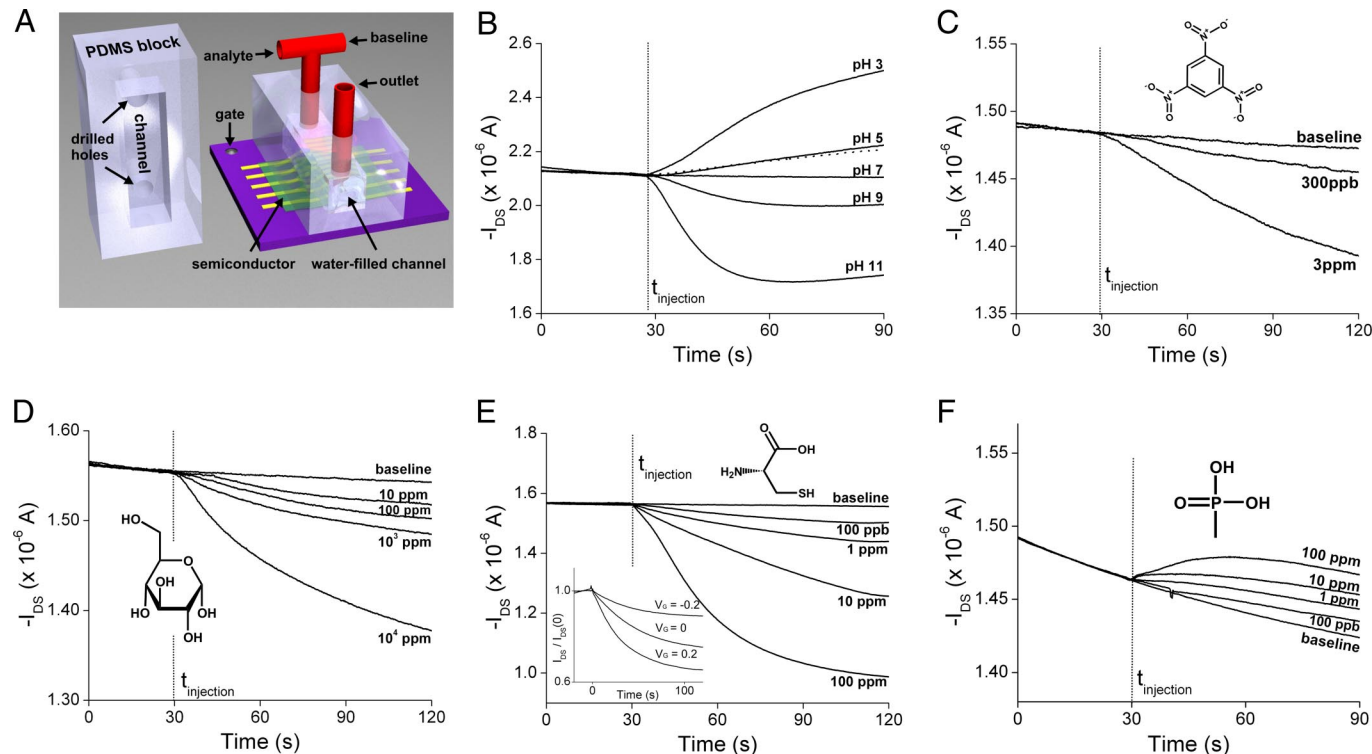


**Fig. 4.** Chemical detection in aqueous systems based on OTFTs ( $V_G = -1$  V,  $V_{DS} = -0.6$  V). (A) Schematic showing an OTFT with DDFTTF in flow cell for aqueous-phase sensing. (B) Drain current,  $I_{DS}$ , response of a DDFTTF OTFT to pH.  $I_{DS}$  response curves for the pH 5 solution were measured before (solid) and after (dashed) the exposure to other pH solutions. (C–F)  $I_{DS}$  response to different analytes: trinitrobenzene (TNB) (C), glucose (D), cysteine (E), and methylphosphonic acid (MPA) (F). (E Inset)  $I_{DS}$  response for 10-ppm cysteine as a function of  $V_G$ . The magnitude of the change in current, referenced to the drain current at time 0 s (the baseline current varies with  $V_G$ ), increases as  $V_G$  is changed from 0.2 to  $-0.2$  V.

presence of water, but their performance was either inadequate (e.g., very low on/off ratio) or degraded too rapidly for use in sensors. For example, OTFTs based on pentacene degrade when biased under water, even at very low voltages ( $<1$  V). We attribute this to either electrochemical damage to the semiconductor or water trapped at the dielectric interface rather than delamination because no change in film morphology was observed by AFM (Fig. S8) (32, 33). Additionally, low-mobility organic semiconductors, including CuPc and FCuPc, generate a low “on” current, which is on the order of the ionic current through the water for a given source-drain bias; hence, little or no gate dependence was observed. Crystalline films of 4TMS showed acceptable device characteristics initially, but the film quickly delaminated under water. It should be stressed that OTFT operation under water is not limited to just FTF-type molecules. We believe that it is desirable for the active layer material to contain long aliphatic side groups to facilitate a close-packed hydrophobic top surface of the semiconducting layer.

The next challenge addressed is the ability to detect dilute analytes in water in the presence of the background current. For sensor applications, selectivity will eventually be realized by using OTFTs as the readout devices in conjunction with a chemical selective membrane or binding layer. Therefore, it is most important that a well defined electrical current change is observed upon exposure to the analyte. As a demonstration of concept, we fabricated a flow cell system directly on the surface of an OTFT comprising a PVP-DPA (22 nm) gate dielectric with DDFTTF (40 nm) as shown in Fig. 4A. The source-drain electrodes ( $W = 4$  mm,  $L = 50$   $\mu\text{m}$ ) in the channel region were coated with 50 nm of thermally evaporated silicon monoxide to reduce the influence of charge screening on the source-drain

current. A baseline of drain current with time was established with deionized water at a flow rate of  $\approx 1$  ml/min under a constant source-drain bias,  $V_{DS} = -0.6$  V, and a constant gate bias,  $V_G = -1$  V. As observed in nearly all organic devices, a slight drift in the source-drain current was observed with time due to gate bias stress (34); however, the initial current was restored after removal of the gate bias. The drain current response curves were normalized by subtraction to the baseline current before the analyte injection.

The influence of pH on the drain current was examined to understand how water influences the electrical behavior of the organic semiconductor. The increase in current observed when the devices are operated under water could be attributed to exposure to either hydronium ( $\text{H}_3\text{O}^+$ ) or hydroxide ions ( $\text{OH}^-$ ). Fig. 4B shows that the drain current increases with decreasing pH (increasing  $[\text{H}_3\text{O}^+]$ ). We conclude that the current change is directly related to the  $\text{H}_3\text{O}^+$  concentration for a few reasons. First, only a negligible change in  $I_{DS}$  is observed for a 1 mM NaCl solution (Fig. S10). In addition,  $I_{DS}$  remains nearly unchanged upon switching to pH solutions in the absence of a gate bias, indicating that the current response is not due to a change in ionic conductivity. In the absence of the gate field,  $\text{H}_3\text{O}^+$  ions are not attracted to the channel region; therefore,  $I_{DS}$  is the result of a combination of the ionic current through the analyte and the current through the semiconductor film. Because the hydronium ions most likely diffuse into the channel region through the grain boundaries, controlling the morphology of DDFTTF (27) is a potential way to improve response time and sensitivity (13).

The slower response observed for lower pH solutions is likely due to an increasing coulomb blockade (repulsion of hydronium ions by positive charges already populating the channel), reducing the rate of hydronium ion diffusion into the channel. At a

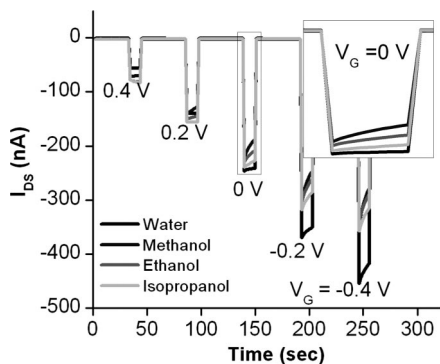


**Fig. 5.** OTFT drain current sensitivity to 1 part per thousand (ppth) solutions of MeOH (dark gray), EtOH (gray), i-PrOH (light gray), and water (black) for  $V_G$  switching on and off (1 V), etc., for "on"  $V_G$  of 0.4, 0.2, 0, -0.2, and -0.4 V. (Inset) Expansion of OTFT drain current from around  $V_G = 0$  V.

higher pH, the  $[H_3O^+]$  concentration gradient is away from the channel and ion diffusion is unobstructed. When the solution is switched from the analyte to water (pH 7), the drain current slowly returns to the initial baseline over a period of 30 s; however, complete recovery requires a reverse gate bias. For inorganic nanowire sensors, the opposite change in  $I_{DS}$  was observed because the protons are believed to assemble at the surface of the oxide and counter the gate field rather than diffusing into the active layer (35, 36).

Despite the presence of ionic current, we found that our OTFTs can still detect the presence of trace amounts of chemicals. Here, we investigated chemical detection of glucose and amino acids, examples of significant biological species. We also tested OTFT sensitivity to analogues of chemical warfare agents, including methylphosphonic acid (MPA) and trinitrobenzene (TNB). MPA represents an analogue of metabolized products of toxic nerve agents, such as Sarin or V-series toxins (2).

A clear drain current response was observed for TNB solutions down to 300 ppb (Fig. 4C). Analytes, such as TNB, most likely act as electronic impurities, introducing traps in the semiconductor film resulting in a decreased drain current. OTFTs were also sensitive to solutions of glucose (Fig. 4D) and cysteine (Fig. 4E) for concentrations over three orders of magnitude down to 10 parts per million (ppm) and 100 ppb, respectively. The basicity of the amine group on the cysteine induces a strong response in the OTFT because of its strong interaction with the hydronium ion dopants and the positive charge carriers. One particular advantage of using a transistor as the readout device as opposed to a simpler two terminal chemresistor is the ability to modulate the drain current with gate bias (37). Indeed, the relative change in the transistor current ( $I_{DS}/I_{DS\text{-baseline}}$ ) depends on the gate bias, as shown in Fig. 4E Inset for a 10-ppm solution of cysteine. Fig. 4F shows the change in drain current for MPA solutions between 100 ppb and 100 ppm.

Similar to vapor sensing with OTFTs, we believe that the sensing mechanism in aqueous media also involves analyte diffusion to the semiconductor/dielectric interface resulting in an influence in the charge transport of the active layer via trapping and doping. To demonstrate the importance of the analyte diffusion through the semiconductor grain boundaries, we investigated the OTFT drain current sensitivity to solutions of alcohols with increasing size. The influence of these analytes (methanol, ethanol, and isopropyl alcohol) on the OTFT drain current was evaluated at various gate voltages. Fig. 5 shows the drain current vs. time for an OTFT saturated with water or 1 part per thousand (ppth) alcohol solutions when the device is switched "off" (1 V) and "on" with an increasingly negative  $V_G$ . As expected, we observe the greatest decrease in current relative

to the baseline for the smallest analyte, methanol, followed by ethanol and then isopropanol. The smaller analyte molecule can diffuse most rapidly through the grain boundaries and exchange with the most number of water molecules at the dielectric interface. Interestingly, the difference in transistor "on" current for the various solutions shows the largest variation at a gate bias below the saturation regime. As the bias is increased beyond this point, the difference between the alcohol solutions becomes negligible. The ability to modulate the  $I_{DS}$  with  $V_G$  improves the sensitivity of these devices. While the detailed sensing mechanism is still under investigation for OTFTs in any media, in this work, the OTFT response is complicated by the presence of water molecules and ions at the surface of the semiconductor. In addition to the analyte acting as an electronic trap, the species must displace a molecule occupying a site. Furthermore, the analyte may also complex with ions in water, thus affecting the local electrostatic environment at the interface. These factors require more extensive studies to deconvolute the various interactions and determine the mechanistic details. Nevertheless, the fact that OTFTs can indeed sense chemicals down to the parts per billion level in aqueous solutions indicates that they can be used as the readout devices in conjunction with a polymer membrane or binding coatings for selective chemical detection in water.

With the demonstration of stable operation in aqueous media, we have overcome a major hurdle for OTFT sensors using low-voltage devices with a stable organic semiconductor. We have shown that the drain current is sensitive to a variety of analytes at concentrations as low as parts per billion. Sensing is achieved in a similar manner as vapor systems, such that small analyte molecules or ions can diffuse to the semiconductor-dielectric interface through grain boundaries within the film and influence the charge transport in the active layer (13). The detailed mechanism is subject to further studies. Nevertheless, this work demonstrates the feasibility of using OTFTs for aqueous sensing applications.

## Materials and Methods

**Materials.** All materials were used as received from Aldrich unless otherwise stated. Pentacene was purified by temperature gradient sublimation in a three-zone furnace ( $10^{-6}$  Torr, 220°C). Poly(4-vinylphenol) (PVP) from Aldrich had an  $M_w$  of 20,000.

**Dielectric Film Preparation.** Solutions of PVP were prepared with a cross-linking agent (either HDA or SC) in a molar ratio of 10:1 based on the PVP monomer in PGMEA. The concentration of PVP was varied between 10 and 50 mg/ml. The solutions were filtered through a 0.2- $\mu$ m syringe filter and spin-coated onto highly doped  $n^{++}$  Si(100) substrates ( $R < 0.008$  ohm-cm) at rates of 3,000–7,000 rpm for 1 min on a spin-coater (Headway Research). Before spin-coating, the substrates were treated with UV-ozone (Jelight Model 42) for 20 min and blown dry with filtered nitrogen (Mykrolis). The substrates were then cured at 100°C for 2 h. The film thickness was determined by using ellipsometry (Optrel Multiscopie at a 70° angle of incidence under nulling conditions with a 532-nm laser with a beam diameter and spot size of 0.6 mm and 20 mV, respectively) and atomic force microscopy (AFM) (Digital Instruments NanoScope IV) operated in tapping mode ( $\approx 300$ -kHz frequency, Si tip).

**OTFT Fabrication.** Semiconductor films were deposited by thermal evaporation (Angstrom Engineering) at a rate of 0.3–0.5 Å/s under a pressure of  $5.0 \times 10^{-7}$  Torr. The substrate temperature ( $T_{\text{sub}}$ ) was controlled by heating a copper block during deposition. Pentacene, DDFTF, and FCuPc were deposited at  $T_{\text{sub}}$  of 65°C, 90°C, and 105°C, respectively, to a thickness of 40 nm. The top-contact devices were completed with gold electrodes thermally evaporated at 1 nm/s with a rotating substrate. Electrode dimensions were defined by a shadow mask with a channel width ( $W$ ) and length ( $L$ ) of 1 mm and 50  $\mu$ m, respectively. For sensor OTFTs, a 50-nm layer of silicon monoxide was thermally evaporated on the electrodes in the channel region.

**Electrical Characterization.** The electrical measurements were carried out in ambient by using a Keithley 4200SCS semiconductor parameter analyzer and a standard probe station setup. Voltage-dependant capacitance measure-

ments were performed by using a Hewlett-Packard 4192 LF Impedance Analyzer for frequencies ranging between 10 Hz and 100 KHz.

**Synthesis.** NMR spectra were recorded on a Varian Mercury 400-MHz spectrometer. Chemical shifts ( $\delta$ ) are reported in parts per million, and the residual solvent peak was used as an internal standard.

**Trimethyl-[2,2',5',2'']quaterthiophen-5-yl-silane (4TTMS).** To a nitrogen-flushed, two-neck flask was added 5-bromo-[2,2']bithiophene (0.49 g, 1.99 mmol) and trimethyl-(5'-tributylstannanyl-[2,2']bithiophenyl-5-yl)-silane (1.0 g, 1.90 mmol) in 20 ml of anhydrous dimethylformamide. The solution was degassed by using freeze-pump-thaw until no gas evolved. [1,1'-Bis(diphenylphosphino)ferrocene]dichloropalladium(II) (77 mg, 0.095 mmol) was added, and the reaction mixture was heated to 90°C for 24 h. After cooling to room temperature, the mixture was poured into methanol and the precipitate was filtered. The crude product was flashed through silica gel in chloroform (566 mg, 74%). The product was further purified by temperature gradient sublimation at  $10^{-6}$  Torr and collected at  $\approx 160^\circ\text{C}$ .  $^1\text{H NMR}$  ( $\text{CDCl}_3$ , 400 MHz):  $\delta_{\text{H}}$  7.23 (d,  $J = 3.6$  Hz, 2 H), 7.18 (d,  $J = 4.0$  Hz, 1 H), 7.14 (d,  $J = 3.6$  Hz, 1 H), 7.07–7.10 (m, 4 H), 7.03 (dd,  $J = 4.8$ ,  $J = 4.8$  Hz, 1 H), 0.33 (s, 9 H). MS (DEI)  $m/z$ : 403 (M<sup>+</sup>).

**Trimethyl-(5'-tributylstannanyl-[2,2']bithiophenyl-5-yl)-silane.** To a nitrogen-flushed flask was added [2,2']bithiophene (10.34 g, 62.19 mmol) in 100 ml of anhydrous tetrahydrofuran. The solution was bubbled with nitrogen for 30 min and then cooled to  $-78^\circ\text{C}$ . *n*-BuLi (12.69 g, 62.65 mmol) was added

drop-wise over 30 min, and the mixture was stirred for 1.5 h and then brought to 25°C. After stirring for 30 min, chlorotrimethylsilane (6.76 g, 62.19 mmol) was added portion-wise and the mixture was stirred for 2 h. The reaction mixture was again cooled to  $-78^\circ\text{C}$ , and *n*-BuLi (12.69 g, 62.65 mmol) was added drop-wise over 15 min. The mixture was stirred for 1 h and then allowed to warm to 25°C for 1 h followed by quenching with tributyltin chloride (20.39 g, 62.65 mmol). The mixture was allowed to stir overnight and then poured into 250 ml of hexanes. The solution was washed with 125 ml of 5%  $\text{NH}_4\text{Cl}$  ( $3\times$ ) and  $\text{H}_2\text{O}$  ( $3\times$ ). The solution was dried over  $\text{MgSO}_4$  and then the solvent was removed by evaporation at reduced pressure.  $^1\text{H NMR}$  ( $\text{CDCl}_3$ , 400 MHz):  $\delta_{\text{H}}$  7.32 (dd,  $J = 3.2$  Hz,  $J = 2.4$  Hz, 1 H), 7.25 (dd,  $J = 3.2$  Hz,  $J = 3.2$  Hz, 1 H), 7.14 (dd,  $J = 3.2$  Hz,  $J = 1.6$  Hz, 1 H), 7.08 (dd,  $J = 3.2$  Hz,  $J = 2.0$  Hz, 1 H), 1.56–1.64 (pent.,  $J = 7.6$  Hz, 6 H), 1.32–1.41 (sext.,  $J = 7.2$  Hz, 6 H), 7.12–7.16 (t,  $J = 7.6$  Hz, 6 H), 0.91–0.94 (t,  $J = 7.6$  Hz, 9 H), 0.34 (s, 9 H).

**ACKNOWLEDGMENTS.** We thank Dr. Edwin Chandross and Dr. Stacey Bent for helpful comments and suggestions. M.E.R. acknowledges partial financial support from a National Aeronautics and Space Administration Graduate Student Research Program Fellowship. S.C.B.M. acknowledges financial support from Deutsche Forschungsgemeinschaft Grant MA 3342/1-1. Z.B. acknowledges financial support from the Stanford Center for Polymeric Interfaces and Macromolecular Assemblies (National Science Foundation–Materials Research Science and Engineering Center), a 3M Faculty Award, a Sloan Research Fellowship, and the Finmeccanica Faculty Scholar Fund.

- Johnson KS, Needoba JA, Riser SC, Showers WJ (2007) Chemical sensor networks for the aquatic environment. *Chem Rev* 107:623–640.
- Voiculescu I, et al. (2006) Micropreconcentrator for enhanced trace detection of explosives and chemical agents. *IEEE Sens J* 6:1094–1104.
- Wang L, et al. (2006) Nanoscale organic and polymeric field-effect transistors as chemical sensors. *Anal Bioanal Chem* 384:310–321.
- Carlen ET, van den Berg A (2007) Nanowire electrochemical sensors: Can we live without labels? *Lab Chip* 7:19–23.
- Janata J, Josowicz M (2003) Conducting polymers in electronic chemical sensors. *Nat Mater* 2:19–24.
- Katz HE (2004) Chemically sensitive field-effect transistors and chemiresistors: New materials and device structures. *Electroanalysis* 16:1837–1842.
- Mabeck JT, Malliaras GG (2006) Chemical and biological sensors based on organic thin-film transistors. *Anal Bioanal Chem* 384:343–353.
- Locklin J, Roberts ME, Mannsfeld SCB, Bao Z (2006) Optimizing the thin film morphology of organic field-effect transistors: The influence of molecular structure and vacuum deposition parameters on device performance. *J Macromol Sci Polymer Rev* 46:79–101.
- Crone B, et al. (2001) Electronic sensing of vapors with organic transistors. *Appl Phys Lett* 78:2229–2231.
- Torsi L, Dodabalapur A, Sabbatini L, Zamboni PG (2000) Multi-parameter gas sensors based on organic thin-film-transistors. *Sens Actuators B* 67:312–316.
- Guo XF, et al. (2006) Chemo-responsive monolayer transistors. *Proc Natl Acad Sci USA* 103:11452–11456.
- Torsi L, et al. (2002) Correlation between oligothiophene thin film transistor morphology and vapor responses. *J Phys Chem B* 106:12563–12568.
- Someya T, et al. (2002) Vapor sensing with  $\alpha,\omega$ -dihexylquaterthiophene field-effect transistors: The role of grain boundaries. *Appl Phys Lett* 81:3079–3081.
- Huang J, Miraghiotta J, Becknell A, Katz HE (2007) Hydroxy-terminated organic semiconductor-based field-effect transistors for phosphonate vapor detection. *J Am Chem Soc* 129:9366–9376.
- Torsi L, et al. (2008) A sensitivity-enhanced field-effect chiral sensor. *Nat Mater* 7:412–417.
- Someya T, et al. (2002) Integration and response of organic electronics with aqueous microfluidics. *Langmuir* 18:5299–5302.
- Qiu Y, et al. (2003)  $\text{H}_2\text{O}$  effect on the stability of organic thin-film field-effect transistors. *Appl Phys Lett* 83:1644–1646.
- Bartici C, Campitelli A, Borghs S (2003) Field-effect detection of chemical species with hybrid organic/inorganic transistors. *Appl Phys Lett* 82:475–477.
- Chua LL, Ho PKH, Sirringhaus H, Friend RH (2004) High-stability ultrathin spin-on benzocyclobutene gate dielectric for polymer field-effect transistors. *Appl Phys Lett* 84:3400–3402.
- Yoon MH, Yan H, Facchetti A, Marks TJ (2005) Low-voltage organic field-effect transistors and inverters enabled by ultrathin cross-linked polymers as gate dielectrics. *J Am Chem Soc* 127:10388–10395.
- Halik M, et al. (2004) Low-voltage organic transistors with an amorphous molecular gate dielectric. *Nature* 431:963–966.
- Yoon MH, Facchetti A, Marks TJ (2005)  $\sigma$ - $\pi$  molecular dielectric multilayers for low-voltage organic thin-film transistors. *Proc Natl Acad Sci USA* 102:4678–4682.
- Klauk H, Zschieschang U, Pflaum J, Halik M (2007) Ultralow-power organic complementary circuits. *Nature* 445:745–748.
- Klauk H, et al. (2002) High-mobility polymer gate dielectric pentacene thin film transistors. *J Appl Phys* 92:5259–5263.
- Halik M, et al. (2002) Polymer gate dielectrics and conducting-polymer contacts for high-performance organic thin-film transistors. *Adv Mater* 14:1717–1722.
- Meng H, et al. (2003) Oligofluorene-thiophene derivatives as high-performance semiconductors for organic thin film transistors. *Chem Mater* 15:1778–1787.
- DeLongchamp DM, et al. (2006) Thickness dependence of microstructure in semiconducting films of an oligofluorene derivative. *J Am Chem Soc* 128:16579–16586.
- Katz HE, et al. (2004) Mesophase transitions, surface functionalization, and growth mechanism of semiconducting 6PTTP6 films from solution. *J Phys Chem B* 108:8567–8571.
- Locklin J, et al. (2005) Organic thin film transistors based on cyclohexyl-substituted organic semiconductors. *Chem Mater* 17:3366–3374.
- Backlund TG, et al. (2005) Operating principle of polymer insulator organic thin-film transistors exposed to moisture. *J Appl Phys* 98:074504.
- Jung T, Dodabalapur A, Wenz R, Mohapatra S (2005) Moisture induced surface polarization in a poly(4-vinyl phenol) dielectric in an organic thin-film transistor. *Appl Phys Lett* 87:182109.
- Li DW, et al. (2005) Humidity effect on electrical performance of organic thin-film transistors. *Appl Phys Lett* 86:042105.
- Zhu ZT, Mason JT, Dieckmann R, Malliaras GG (2002) Humidity sensors based on pentacene thin-film transistors. *Appl Phys Lett* 81:4643–4645.
- Zilker SJ, Detchervey C, Cantatore E, de Leeuw DM (2001) Bias stress in organic thin-film transistors and logic gates. *Appl Phys Lett* 79:1124–1126.
- Cui Y, Wei QQ, Park HK, Lieber CM (2001) Nanowire nanosensors for highly sensitive and selective detection of biological and chemical species. *Science* 293:1289–1292.
- Stern E, et al. (2007) Label-free immunodetection with CMOS-compatible semiconducting nanowires. *Nature* 445:519–522.
- Tanese MC, Fine D, Dodabalapur A, Torsi L (2005) Interface and gate bias dependence responses of sensing organic thin-film transistors. *Biosens Bioelectron* 21:782–788.